



CHAOTIC VARIANTS OF THE PSO-SRM FOR OPTIMUM DESIGN OF THE STEEL FRAMES

A. Kaveh^{*†} and A. Zaerreza

School of Civil Engineering, Iran University of Science and Technology, P.O. Box 16846-13114, Iran

ABSTRACT

This paper presents the chaotic variants of the particle swarm optimization-statistical regeneration mechanism (PSO-SRM). The nine chaotic maps named Chebyshev, Circle, Iterative, Logistic, Piecewise, Sine, Singer, Sinusoidal, and Tent are used to increase the performance of the PSO-SRM. These maps are utilized instead of the random number, which defines the solution generation method. The robustness and performance of these methods are tested in the three steel frame design problems, including the 1-bay 10-story steel frame, 3-bay 15-story steel frame, and 3-bay 24-story steel frame. The optimization results reveal that the applied chaotic maps improve the performance of the PSO-SRM.

Keywords: Chaotic maps, structural optimization, Particle swarm optimization-statistical regeneration mechanism, steel structures, metaheuristic algorithms.

Received: 10 January 2023 Accepted: 16 April 2023

1. INTRODUCTION

Due to resource limitations, the optimum design of the structure has been the most popular research item in the last four decades [1, 2]. Gradient-based methods and metaheuristic algorithms are two well-known optimization methods. Metaheuristic algorithms are easily coded and do not need gradient information [3, 4]. Hence, metaheuristic algorithms are popular optimization methods for optimizers. Therefore, metaheuristic algorithms are used by the structural optimizer in the different optimization problems.

A single optimization method cannot solve all kinds of optimization problems efficiently. Hence, researchers have invented different optimization methods [5]. Some of the new of

^{*}Corresponding author: School of Civil Engineering, Iran University of Science and Technology, P.O. Box 16846-13114, Iran

[†]E-mail address: alikaveh@iust.ac.ir (A. Kaveh)

them can refer to, Across Neighbourhood Search (ANS) introduced by Wu [6], Andean Condor Algorithm presented by Almonacid and Soto [7], Artificial Electric Field Algorithm (AEEA) developed by Anita and Yadav [8], Cheetah Based Algorithm (CBA) introduced by Klein et al [9], Coyote optimization algorithm (COA) developed by Pierezan and Coelho [10], Emperor Penguins Colony (EPC) presented by Harifi et al. [11], Flow Regime Algorithm (FRA) presented by Tahani and Babayan [12], Hunger Games Search (HGS) developed by Yang et al. [13], Monarch Butterfly Optimization (MBO) introduced by Wang et al. [14], Newton Metaheuristic Algorithm (NMA) developed by Gholizadeh et al. [15], Lion algorithm (LA) is introduced by Rajakumar [16], Pity Beetle Algorithm (PBA) developed by Kallioras et al. [17], Shuffled shepherd optimization algorithm (SSOA) presented by Kaveh and Zaerreza [18], Squirrel Search Algorithm (SSA) developed by Jain et al. [19], Team Game Algorithm (TGA) presented by Mahmoodabadi et al. [20], and Queuing search algorithm (QSA) developed by Zhang et al. [21].

In the field of structural optimization, metaheuristic algorithms are used by different researchers for their optimization problems, such as Kaveh and Talatahari [22] applied the enhanced charged system search in the configuration optimization problem. Mohebian et al. [23] utilized differential evolution (DE) in the structural damage detection problem. Al Thobiani et al. [24] applied the hybrid version of the PSO and gray wolf optimization method to the crack detection problem. Kaveh and Rahami [25] utilized the genetic algorithm for the optimum design of the structures. Kazemzadeh Azad et al. [26] developed the upper-bound strategy framework for the optimum design of structures using metaheuristic algorithms. Alkayem et al. [27] presented a new enhanced version of the PSO for the structural damage detection problem.

One of the efficient ways to improve the performance of meta-heuristic algorithms is by applying chaotic maps [28]. In the metaheuristic algorithms, chaotic maps are used instead of the random number in the main cycle of the optimization methods. Some of the recent applications of chaotic maps in improving the metaheuristic algorithms are listed as follows. Talatahari et al. [29] applied chaotic maps to improve the performance of the charged system search algorithms. Kaveh and Yousefpoor [30] developed enhanced metaheuristic algorithms using chaotic maps for the optimum design of the truss. Gharehchopogh et al. [31] developed the chaotic vortex search for future selection. Das and Saha [32] applied chaotic maps to structural health monitoring problems. Talatahari et al. [33] presented the chaotic imperialist competitive algorithm for the optimum design of the structure. Kaveh and Javadi [34] developed the chaotic firefly algorithms for the optimum design of large-scale structures.

This paper presents the chaotic variant of the particle swarm optimization-statistical regeneration mechanism (PSO-SRM). For this purpose, nine chaotic maps are considered, including the Chebyshev, Circle, Iterative, Logistic, Piecewise, Sine, Singer, Sinusoidal, and Tent. These maps are used instead of the random number, which defines the solution generation method. The efficiency of the chaotic variants of the PSO-SRM is tested in the three steel frames. In these examples, the efficiency of the force method is previously approved by Kaveh and Zaerreza [35]. Therefore, the force method is utilized as the analyzing method. More information about the force method is available in ref [2]. The optimization problem results show that the chaotic maps improve the performance of the PSO-SRM algorithm.

2. PARTICLE SWARM OPTIMIZATION-STATISTICAL REGENERATION MECHANISM (PSO-SRM)

The improved version of the particle swarm optimization algorithms utilizing the statistical regeneration mechanism (SRM) is presented in this section, which is developed by Kaveh and Zaerreza [35]. In the PSO-SRM, the statistical regeneration mechanism is utilized. This mechanism improves the performance of the different optimization methods, such as Rao algorithms[36]. In the PSO-SRM, fifty percent of the solution is generated utilizing the basic particle swarm optimization algorithm, and the remaining solution is generated using the statistical regeneration mechanism (SRM). In order to add the SRM, in the first fifty percent of the optimization cycles, twenty percent variable of the considered solution is regenerated using the SRM. In the remaining iterations, only one variable of the solution is regenerated utilizing the SRM. The steps of the PSO-SRM are provided as follows.

Step 1: Initialization

In the initialization step, the solutions are generated randomly in the search space using Eq (1).

$$P_i^0 = P_{min} + rd \times (P_{max} - P_{min}) \quad i = 1, 2, 3, \dots, n \quad (1)$$

in which P_i^0 is the initial value of the i th particle in the search space. P_{min} and P_{max} are the lower and upper bound of the search space. rd is the random vector generated between 0 and 1. n is the number of the particle, which is defined by the user.

Step 2: Define the new solution generation method

In order to find which solution generation method is utilized, a random number is generated. If the value of the random number is less than α , then the solution is generated using the basic PSO solution generation method, so the algorithm goes to step 3. Otherwise, the statistical regeneration mechanism (SRM) is utilized to generate the new solution, and the algorithms go to step 4.

Step 3: Generate the new solution based on the PSO

The solution generation based on the PSO consists of three components, including the step size of the solution in the previous iteration, moving toward the best solution obtained by the entire population, and moving toward the best solution obtained by the considered solution. Therefore, the new solution is generated utilizing the following equation.

$$P_i^{t+1} = w \times (P_i^t - P_i^{t-1}) + c_1 \times rand_1 \times (P_i^b - P_i^t) + c_2 \times rand_2 \times (P_i^{Gb} - P_i^t) \quad (2)$$

where P_i^{t+1} is the new position of the i th particle in the $t+1$ th iteration. P_i^t and P_i^{t-1} are the positions of the i th particle in the t th and $t-1$ th iteration. P_i^b is the best solution obtained by the considered particle. P_i^{Gb} is the best solution obtained by the whole of the particles. w is the parameter which is the value of it is set to 1 and decreased by 0.01 percent in each

iteration. c_1 and c_2 are user-defined parameters.

Step 4: Generate the new solution using the SRM

In order to generate the new solution using the SRM, the considered solution is replaced with the P_i^b . Then, in the first fifty percent of the iteration, twenty percent variable of the considered solution is selected and regenerated utilizing Eq (3). Otherwise, one variable of the considered solution is selected randomly and regenerated using Eq (3).

$$P_i^{t+1} = U(\text{Mean} - \text{Std} - \text{Sigma}, \text{Mean} + \text{Std} + \text{Sigma}) \quad (3)$$

where U is the operator that returns a random number generated from the continuous uniform distribution with lower and upper endpoints specified by $\text{Mean} - \text{Std} - \text{Sigma}$ and $\text{Mean} + \text{Std} + \text{Sigma}$. Mean and Std are the average and standard deviation of the best solutions found by the particles. Sigma is a parameter that helps the statistically regenerated mechanism to work efficiently when the entire population converges to the specified value and is defined as follows.

$$\text{Sigma} = \begin{cases} 3 & \text{If } \text{Std} < 0.01 \times (P_{\max} - P_{\min}) \\ 0 & \text{otherwise} \end{cases} \quad (4)$$

The value of the 3 is considered for the Sigma by testing the different functions and values. Due to using the rounding function to connect the discrete optimization problem to continuous optimization methods, using the constant value of the 3 it means that in Eq (3) at least 3 bigger or smaller sections than Mean are selected.

Step 5: Check the termination condition

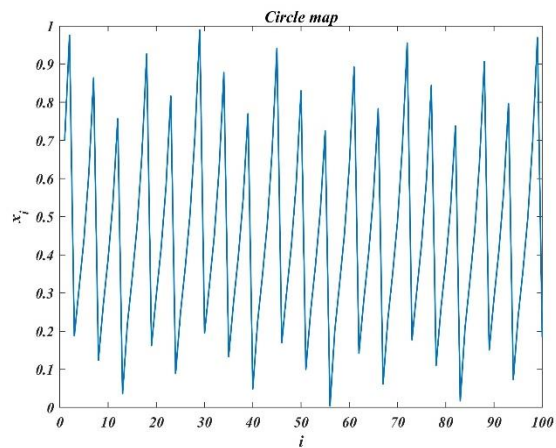
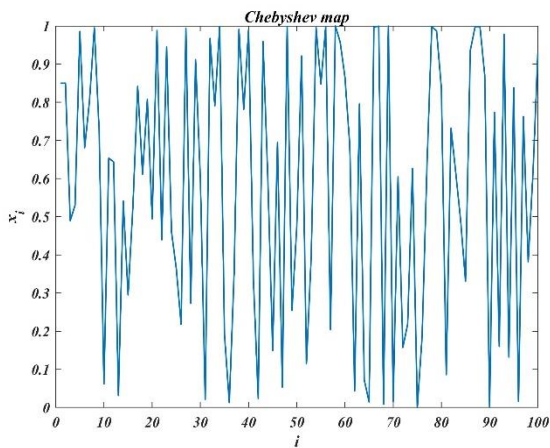
The maximum number of iterations is considered as the termination condition of the algorithm. If the termination condition is satisfied, the optimization process is stopped, and the P_i^{Gb} is reported. Otherwise, the algorithm goes to Step 2 for the next cycle of optimization.

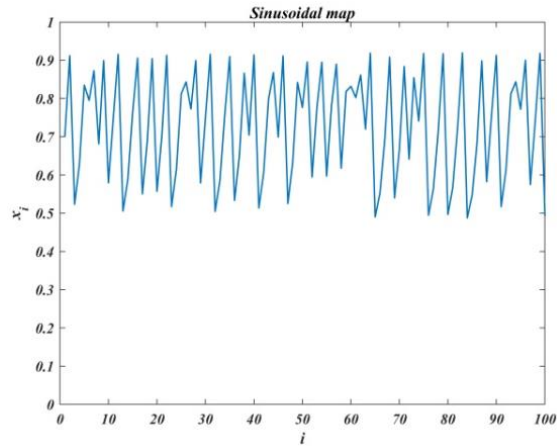
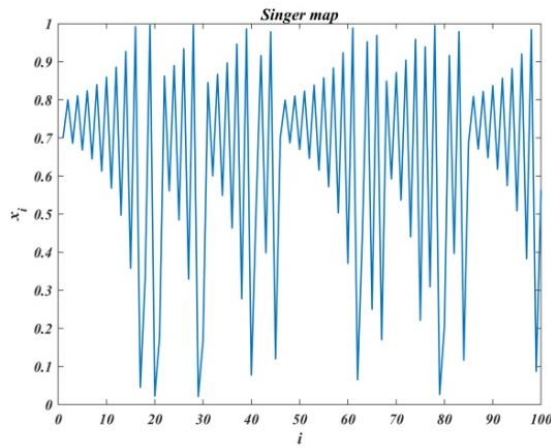
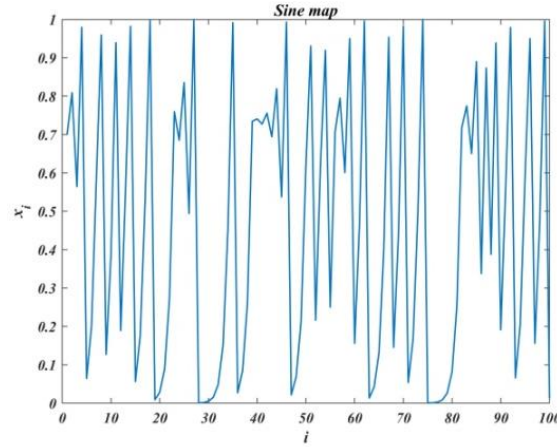
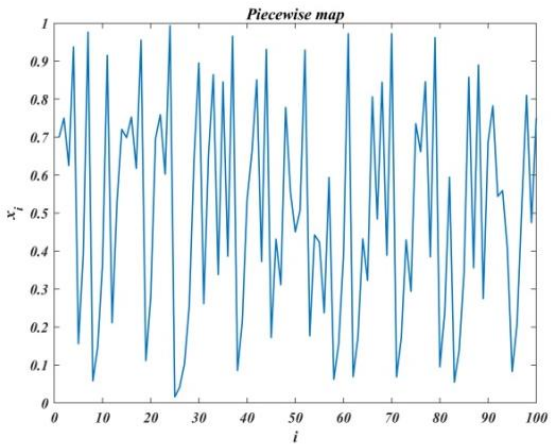
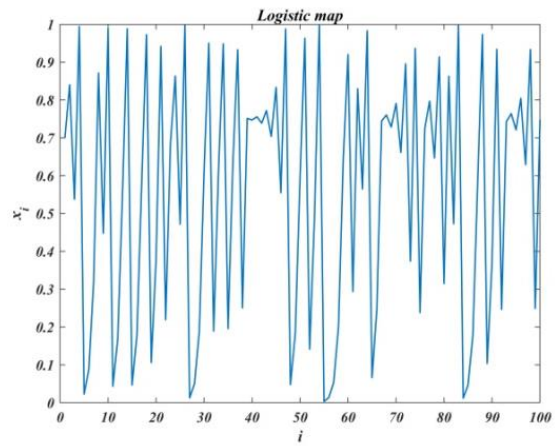
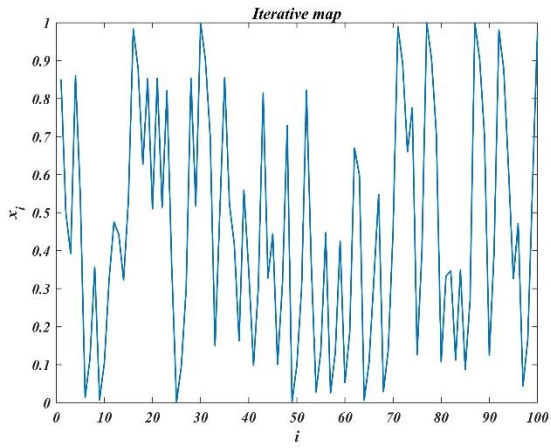
3. CHAOTIC PARTICLE SWARM OPTIMIZATION-STATISTICAL REGENERATION MECHANISM

In this study, nine chaotic maps are considered, and the performance of PSO-SRM is investigated using these maps. These maps include the Chebyshev [37], Circle [38], Iterative[39], Logistic[39], Piecewise[40], Sine[41], Singer [42], Sinusoidal [43], Tent[44]. These maps are used in step 2 of the PSO-SRM. In step 2, the chaotic maps are utilized instead of the random number. Therefore, there are nine different variants of the PSO-SRM provided in this study. The name of the algorithms using these maps and the mathematical formulation of the chaotic maps are provided in Table (1), and visualization of them is provided in Figure 1.

Table 1. Formulation of the chaotic maps

| Name of map | Name of the algorithm using the map | Chaotic map |
|-------------|-------------------------------------|---|
| Chebyshev | ChPSO-SRM | $x_{i+1} = \cos(i \cos^{-1}(x_i))$ |
| Circle | CiPSO-SRM | $x_{i+1} = \text{mod} \left(x_i + 0.2 - \left(\frac{0.5}{2\pi} \right) \sin(2\pi x_k), 1 \right)$ |
| Iterative | IPSO-SRM | $x_{i+1} = \sin \left(\frac{0.7\pi}{x_i} \right)$ |
| Logistic | LPSO-SRM | $x_{i+1} = 4x_i(1 - x_i)$ |
| Piecewise | PiPSO-SRM | $x_{i+1} = \begin{cases} \frac{x_i}{P} & 0 \leq x_i < P \\ \frac{x_i - P}{0.5 - P} & P \leq x_i < 0.5 \\ \frac{1 - P - x_i}{0.5 - P} & 0.5 \leq x_i < 1 - P \\ \frac{1 - x_i}{P} & 1 - P \leq x_i < 1 \end{cases}, P = 0.4$ |
| Sine | SinePSO-SRM | $x_{i+1} = \frac{a}{4} \sin(\pi x_i), a = 4$ |
| Singer | SingPSO-SRM | $x_{i+1} = \mu(7.86x_i - 23.31x_i^2 + 28.75x_i^3 - 13.302875x_i^4),$ $\mu = 1.07$ |
| Sinusoidal | SinuPSO-SRM | $x_{i+1} = ax_i^2 \sin(\pi x_i), a = 2.3$ |
| Tent | TPSO-SRM | $x_{i+1} = \begin{cases} x_i & x_i < 0.7 \\ \frac{10}{3}(1 - x_i) & x_i \geq 0.7 \end{cases}$ |





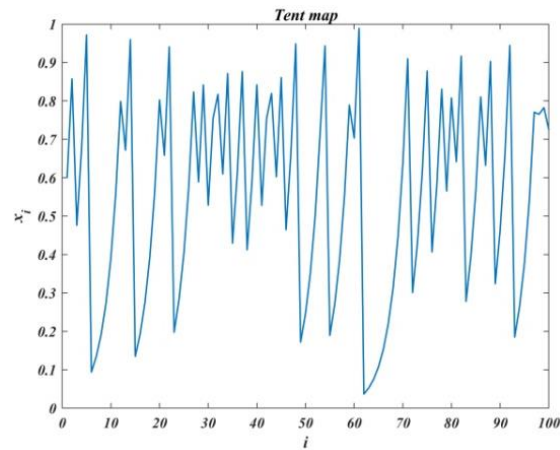


Figure 1. Behaviour of the chaotic maps

4. NUMERICAL EXAMPLES

Three 2D steel frame is considered in this study to investigate the performance of the chaotic variants of the PSO-SRM. These examples are 1-bay 10-story steel frame, 3-bay 15-story steel frame, and 3-bay 24-story steel frame. In these examples, AISC-LRFD requirements are fulfilled for the stress and displacement limitation. The population size is 20, and the maximum number of function evaluations is 20000. c_1 and c_2 are set to 2 in all of the variants of the PSO-SRM. α is set to 0.8 in the chaotic variants of the PSO-SRM, and α is set to 0.5 in the basic PSO-SRM algorithms.

4.1 The 1-bay 10-story steel frame

The 1-bay 10-story is the first skeletal example considered in this study to examine the performance of the chaotic algorithms, as shown in Figure 2. The members of this structure are divided into the 9 element groups. The section for the beam members is selected from the 267 W-section, and the section for the column elements is selected from W 12 and W 14 sections. The elasticity modulus and yield stress of the members are set to 29000 ksi and 36 ksi, respectively.

The results obtained by the basic algorithms and chaotic variants of the PSO-SRM are provided in Table 2. According to this Table, all chaotic variants of the PSO-SRM can find the optimum result same as the basic algorithms. The worst weight of the 30 independents run of the ChPSO-SRM, CiPSO-SRM, LPSO-SRM, SinuPSO-SRM and TPSO-SRM is better than the basic algorithms. In term of the average weight, only the results of the CiPSO-SRM is worse than basic PSO-SRM. The other chaotic algorithms have better average weights than basic PSO-SRM algorithms. Convergence history for the best and average run of the PSO-SRM and chaotic variants of it is provided in figures 3 and 4.

Table 2. Comparison results of the chaotic variants of PSO-SRM in the 1-bay 10-story steel frame

| Element group | PSO-SRM [35] | ChPSO-SRM | CiPSO-SRM | IPSO-SRM | LPSO-SRM | PiPSO-SRM | SinePS O-SRM | SingPS O-SRM | SinuPS O-SRM | TPSO-SRM |
|---------------|--------------|--------------|--------------|--------------|--------------|--------------|--------------|--------------|--------------|--------------|
| 1 | W14×2 33 | W14×2 33 | W14×2 33 | W14×2 33 | W14×2 33 | W14×2 33 | W14×2 33 | W14×2 33 | W14×2 33 | W14×2 33 |
| 2 | W14×1 76 | W14×1 76 | W14×1 76 | W14×1 76 | W14×1 76 | W14×1 76 | W14×1 76 | W14×1 76 | W14×1 76 | W14×1 76 |
| 3 | W14×1 59 | W14×1 59 | W14×1 59 | W14×1 59 | W14×1 59 | W14×1 59 | W14×1 59 | W14×1 59 | W14×1 59 | W14×1 59 |
| 4 | W14×9 9 | W14×9 9 | W14×9 9 | W14×9 9 | W14×9 9 | W14×9 9 | W14×9 9 | W14×9 9 | W14×9 9 | W14×9 9 |
| 5 | W14×6 1 | W14×6 1 | W14×6 1 | W14×6 1 | W14×6 1 | W14×6 1 | W14×6 1 | W14×6 1 | W14×6 1 | W14×6 1 |
| 6 | W33×1 18 | W33×1 18 | W33×1 18 | W33×1 18 | W33×1 18 | W33×1 18 | W33×1 18 | W33×1 18 | W33×1 18 | W33×1 18 |
| 7 | W30×9 0 | W30×9 0 | W30×9 0 | W30×9 0 | W30×9 0 | W30×9 0 | W30×9 0 | W30×9 0 | W30×9 0 | W30×9 0 |
| 8 | W27×8 4 | W27×8 4 | W27×8 4 | W27×8 4 | W27×8 4 | W27×8 4 | W27×8 4 | W27×8 4 | W27×8 4 | W27×8 4 |
| 9 | W18×4 6 | W18×4 6 | W18×4 6 | W18×4 6 | W18×4 6 | W18×4 6 | W18×4 6 | W18×4 6 | W18×4 6 | W18×4 6 |
| Best (lb) | 64001.9 8 | 64001.9 8 | 64001.9 8 | 64001.9 8 | 64001.9 8 | 64001.9 8 | 64001.9 8 | 64001.9 8 | 64001.9 8 | 64001.9 8 |
| Worst (lb) | 66150.0 2 | 65203.8 2 | 66017.2 4 | 66987.8 3 | 66013.6 3 | 66668.6 2 | 66551.9 8 | 66635.9 6 | 66027.0 9 | 66138.1 1 |
| Mean (lb) | 64607.0 8 | 64328.4 1 | 64672.6 1 | 64561.3 1 | 64473.6 1 | 64389.7 0 | 64558.4 5 | 64545.8 8 | 64541.8 4 | 64319.3 4 |
| SD (lb) | 640.86 | 330.76 | 646.30 | 696.24 | 504.76 | 580.12 | 710.44 | 729.71 | 572.65 | 439.74 |

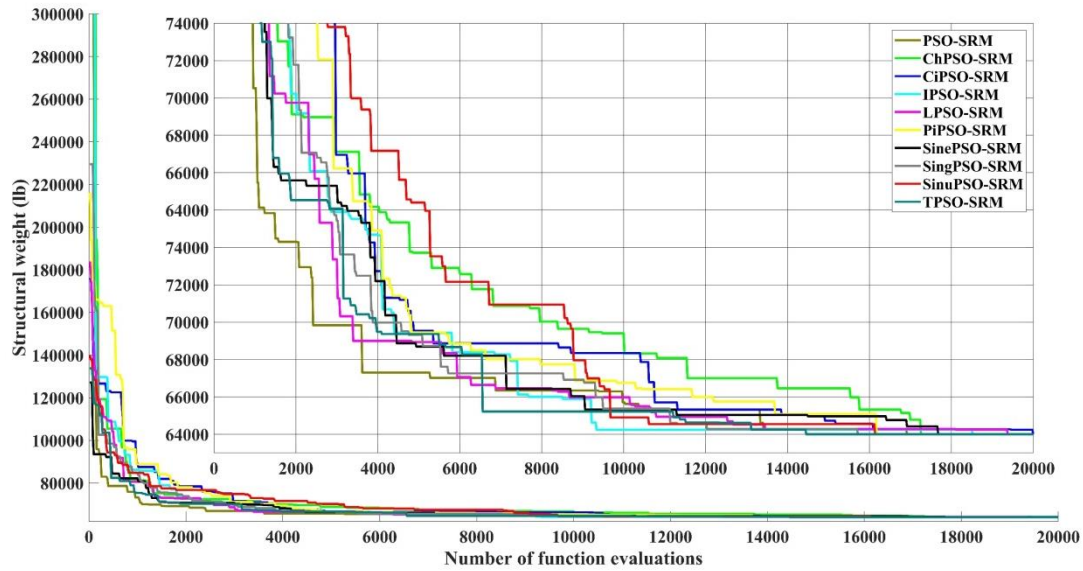


Figure 3. Convergence histories for the best run of the PSO-SRM and chaotic algorithms for the 1-bay 10-story steel frame

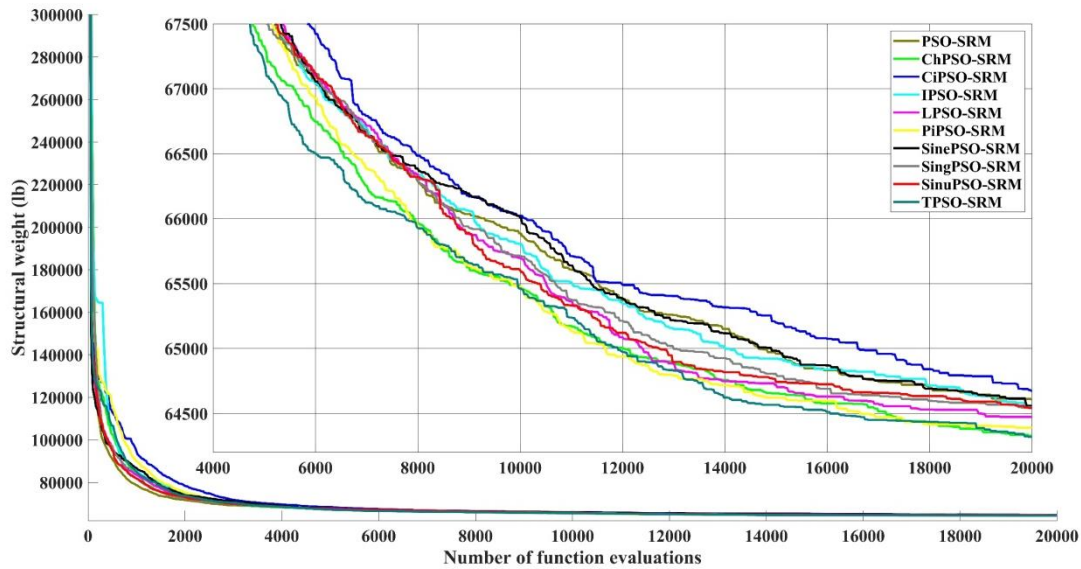


Figure 4. Convergence histories for the average run of the PSO-SRM and chaotic algorithms for the 1-bay 10-story steel frame

4.2 The 3-bay 15-story steel frame

The second example investigated in this study is the 3-bay 15-story steel frame. The structural members of this example are divided into 10 groups for the column member and one group for the beam members, as shown in Figure 5. The section for the beam and column members are picked from the 267 W-section. The elasticity modulus and yield stress of the members are set to 29000 ksi and 36 ksi, respectively. In addition to the AISC-LRFD

requirements, the maximum last story sway is limited to 9.25 in.

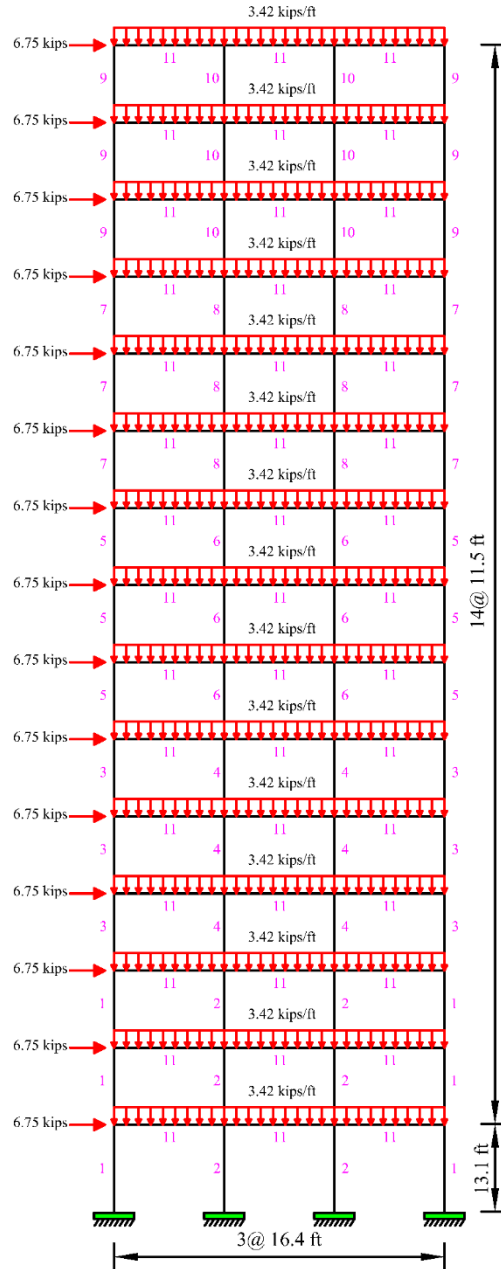


Figure 5. The schematic of the 3-bay 15-story steel frame

The optimization result is summarized in Table 3. According to this Table, SinePSO-SRM obtained a better weight (86916.97 lb) than other considered methods. In addition, the chaotic methods named ChPSO-SRM, CiPSO-SRM, PiPSO-SRM, SinePSO-SRM, SingPSO-SRM, and TPSO-SRM obtained the better result than PSO-SRM. The statistical result obtained by the ChPSO-SRM is better than the basic algorithm. The improvement in

the optimum result and statistical results shows that the chaotic maps considered in this study perfectly enhance the performance of the PSO-SRM. Convergence history for the best and average run of the PSO-SRM and chaotic variants of it is provided in Figs 6 and 7.

Table 3. Comparison results of the chaotic variants of PSO-SRM in the 3-bay 15-story steel frame

| Element group | PSO-SRM [35] | ChPSO-SRM | CiPSO-SRM | IPSO-SRM | LPSO-SRM | PiPSO-SRM | SinePSO-SRM | SingPSO-SRM | SinuPSO-SRM | TPSO-SRM |
|---------------|--------------|-----------|-----------|----------|----------|-----------|-------------|-------------|-------------|----------|
| 1 | W12×96 | W16×89 | W16×89 | W16×89 | W14×99 | W16×89 | W14×90 | W14×99 | W24×94 | W14×99 |
| 2 | W27×16 | W36×17 | W36×17 | W36×17 | W27×16 | W36×17 | W36×17 | W27×16 | W30×17 | W27×16 |
| 3 | W27×84 | W27×84 | W14×82 | W27×84 | W27×84 | W14×82 | W27×84 | W27×84 | W18×76 | W27×84 |
| 4 | W21×11 | W24×10 | W24×10 | W24×10 | W24×10 | W24×10 | W24×10 | W24×10 | W24×11 | W24×10 |
| 5 | W14×61 | W14×61 | W21×68 | W21×68 | W21×68 | W21×68 | W14×61 | W14×61 | W12×58 | W14×61 |
| 6 | W30×90 | W30×90 | W18×86 | W18×86 | W18×86 | W18×86 | W30×90 | W30×90 | W30×90 | W30×90 |
| 7 | W8×48 | W8×48 | W14×48 | W12×45 | W8×48 | W14×48 | W8×48 | W14×48 | W10×45 | W8×48 |
| 8 | W12×65 | W12×65 | W12×65 | W21×68 | W12×65 | W12×65 | W12×65 | W12×68 | W14×68 | W12×65 |
| 9 | W6×25 | W8×28 | W8×28 | W8×28 | W8×28 | W8×28 | W6×25 | W6×25 | W8×24 | W8×28 |
| 10 | W8×40 | W10×39 | W10×39 | W10×39 | W10×39 | W10×39 | W8×40 | W8×40 | W16×40 | W10×39 |
| 11 | W21×44 | W21×44 | W21×44 | W21×44 | W21×44 | W21×44 | W21×44 | W21×44 | W21×44 | W21×44 |
| Best (lb) | 87183.3 | 87054.9 | 87123.9 | 87261.9 | 87261.9 | 87123.9 | 86916.9 | 87123.9 | 87202.5 | 87054.9 |
| Worst (lb) | 88861.7 | 88218.3 | 91956.4 | 88306.5 | 88046.5 | 88604.9 | 88099.5 | 91873.2 | 90775.5 | 91611.4 |
| Mean (lb) | 87606.5 | 87591.3 | 88199.9 | 87709.0 | 87610.6 | 87767.1 | 87572.4 | 87661.3 | 87748.0 | 88102.6 |
| SD (lb) | 318.36 | 291.51 | 1094.61 | 268.92 | 241.13 | 400.05 | 308.66 | 821.26 | 810.33 | 1246.65 |

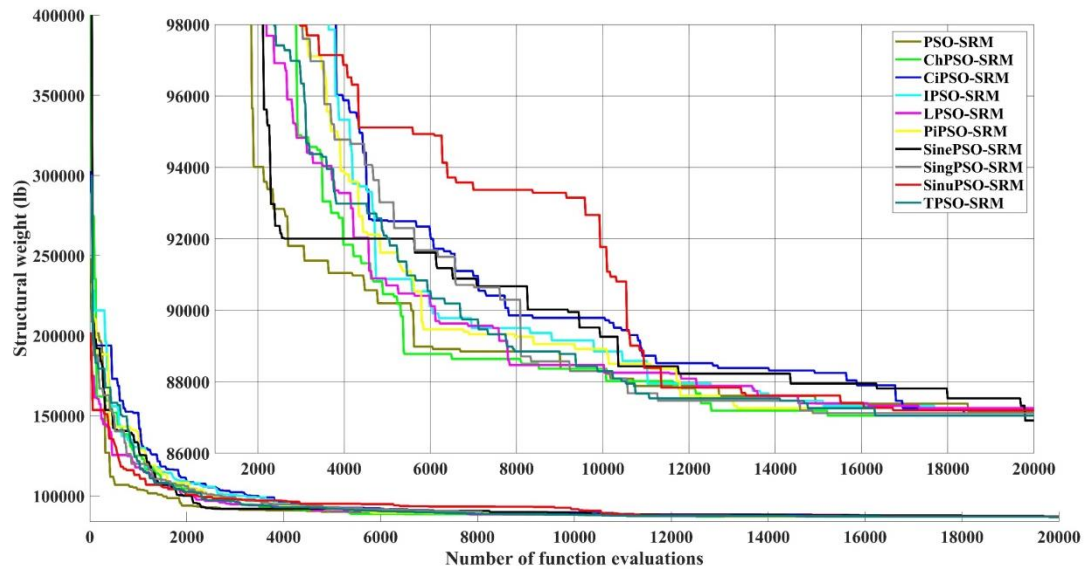


Figure 6. Convergence histories for the best run of the PSO-SRM and chaotic algorithms for the 3-bay 15-story steel frame

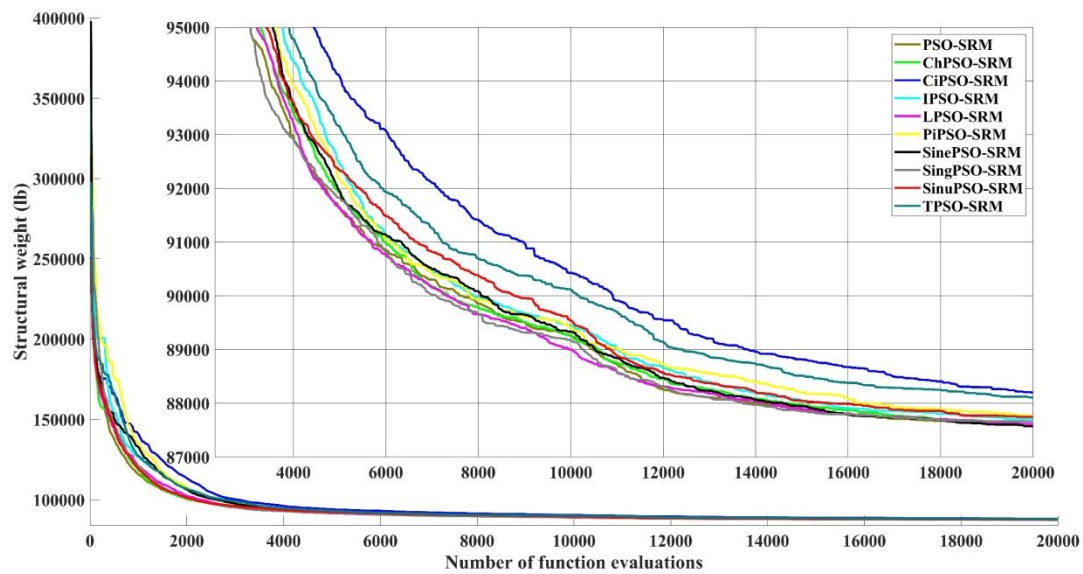


Figure 7. Convergence histories for the average run of the PSO-SRM and chaotic algorithms for the 3-bay 15-story steel frame

4.3 The 3-bay 24-story steel frame

The last example considered in this study to examine the performance of the methods is the 3-bay 15-story steel frame. This frame is made up of 168 members, which are divided into 20 groups, as shown in Figure 8. The section of the column member is selected from W 14 sections, and the beam elements are picked from 267 W sections. The elasticity modulus and yield stress of the members are set to 29732 ksi and 33.4 ksi, respectively.

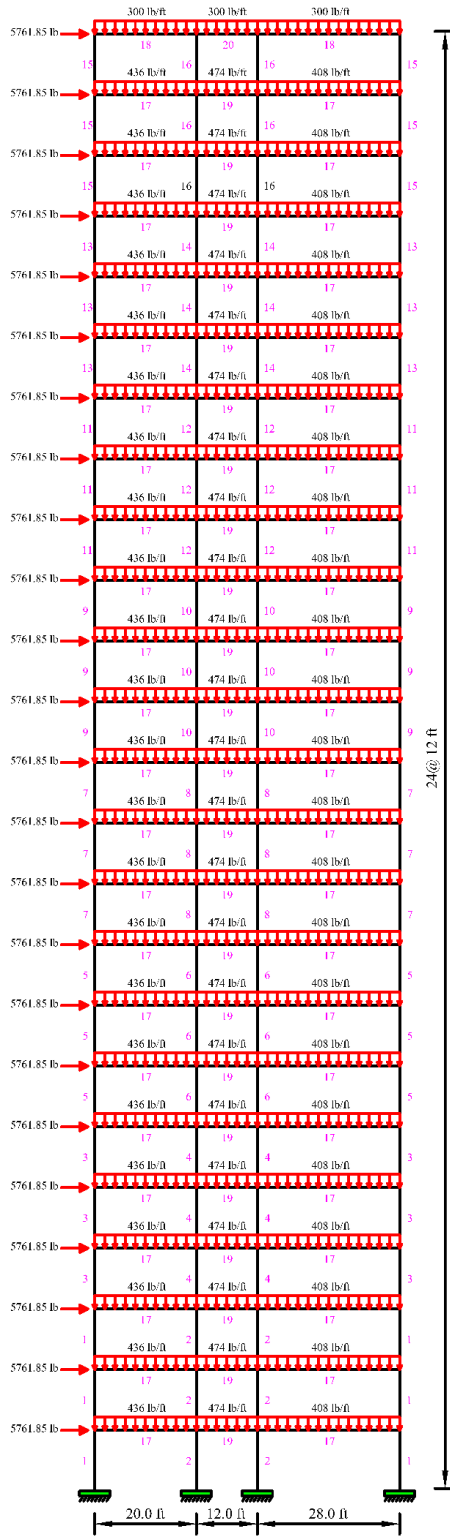


Figure 8. The schematic of the 3-bay 24-story steel frame.

The results of the considered algorithms are provided in Table 4. According to this Table, IPSO-SRM and SingPSO-SRM found the optimum result same as the basic PSO-SRM. However, in terms of the statistical result for the 30 independent runs, IPSO-SRM and SingPSO-SRM acquired better results than PSO-SRM. Convergence history for the best and average run of the PSO-SRM and chaotic variants of it is provided in Figures 9 and 10.

Table 4. Comparison results of the chaotic variants of PSO-SRM in the 3-bay 24-story steel frame

| Element group | PSO-SRM | ChPSO-SRM | CiPSO-SRM | IPSO-SRM | LPSO-SRM | PiPSO-SRM | SinePSO-SRM | SingPSO-SRM | SinuPSO-SRM | TPSO-SRM |
|---------------|-------------|-------------|-------------|-------------|-------------|-------------|-------------|-------------|-------------|-------------|
| 1 | W14×15 9 | W14×15 9 | W14×15 9 | W14×15 9 | W14×14 5 | W14×15 9 | W14×15 9 | W14×15 9 | W14×13 2 | W14×14 5 |
| 2 | W14×13 2 | W14×10 9 | W14×13 2 | W14×13 2 | W14×14 5 | W14×12 0 | W14×13 2 | W14×10 9 | W14×99 | W14×13 2 |
| 3 | W14×10 9 | W14×99 | W14×99 | W14×10 9 | W14×10 9 | W14×10 9 | W14×99 | W14×99 | W14×10 9 | W14×12 0 |
| 4 | W14×74 | W14×82 | W14×74 | W14×74 | W14×74 | W14×74 | W14×74 | W14×82 | W14×90 | W14×74 |
| 5 | W14×82 | W14×74 | W14×82 | W14×68 | W14×61 | W14×68 | W14×61 | W14×74 | W14×74 | W14×61 |
| 6 | W14×48 | W14×53 | W14×38 | W14×38 | W14×43 | W14×43 | W14×43 | W14×43 | W14×38 | W14×43 |
| 7 | W14×30 | W14×34 | W14×48 | W14×38 | W14×38 | W14×34 | W14×38 | W14×38 | W14×34 | W14×34 |
| 8 | W14×22 | W14×22 | W14×22 | W14×22 | W14×22 | W14×22 | W14×22 | W14×22 | W14×22 | W14×22 |
| 9 | W14×90 | W14×90 | W14×90 | W14×90 | W14×99 | W14×99 | W14×90 | W14×90 | W14×99 | W14×99 |
| 10 | W14×99 | W14×10 9 | W14×99 | W14×99 | W14×99 | W14×10 9 | W14×99 | W14×10 9 | W14×12 0 | W14×99 |
| 11 | W14×90 | W14×99 | W14×99 | W14×90 | W14×90 | W14×99 | W14×99 | W14×99 | W14×99 | W14×90 |
| 12 | W14×90 | W14×90 | W14×90 | W14×90 | W14×90 | W14×99 | W14×90 | W14×90 | W14×90 | W14×90 |
| 13 | W14×61 | W14×68 | W14×61 | W14×68 | W14×74 | W14×74 | W14×74 | W14×68 | W14×74 | W14×74 |
| 14 | W14×53 | W14×53 | W14×61 | W14×61 | W14×61 | W14×61 | W14×61 | W14×61 | W14×68 | W14×61 |
| 15 | W14×34 | W14×34 | W14×26 | W14×30 | W14×30 | W14×34 | W14×30 | W14×30 | W14×34 | W14×34 |
| 16 | W14×22 | W14×22 | W14×22 | W14×22 | W14×22 | W14×22 | W14×22 | W14×22 | W14×22 | W14×22 |
| 17 | W30×90 | W30×90 | W30×90 | W30×90 | W30×90 | W30×90 | W30×90 | W30×90 | W30×90 | W30×90 |
| 18 | W6×15 | W6×15 | W6×15 | W6×15 | W6×15 | W8×18 | W6×15 | W6×15 | W6×15 | W8×18 |
| 19 | W24×55 | W24×55 | W24×55 | W24×55 | W24×55 | W14×48 | W24×55 | W24×55 | W24×55 | W24×55 |
| 20 | W6×8.5 | W6×8.5 | W6×8.5 | W6×8.5 | W6×8.5 | W6×8.5 | W6×8.5 | W6×8.5 | W6×8.5 | W6×8.5 |
| Best (lb) | 201402.05 | 201546.04 | 201906.03 | 201402.04 | 201906.05 | 201846.02 | 201583.04 | 201402.04 | 202050.03 | 201906.04 |
| Worst (lb) | 207372.11 | 207793.50 | 225029.82 | 206886.01 | 209981.93 | 216229.13 | 222941.79 | 207158.12 | 215175.79 | 210197.93 |
| Mean (lb) | 203400.11 | 203507.01 | 205918.02 | 203406.27 | 204019.56 | 204760.95 | 204456.12 | 203259.69 | 204462.09 | 204325.57 |
| SD (lb) | 1539.31 | 1512.02 | 4501.81 | 1322.98 | 2143.71 | 2891.80 | 4085.43 | 1242.53 | 2965.53 | 2160.70 |

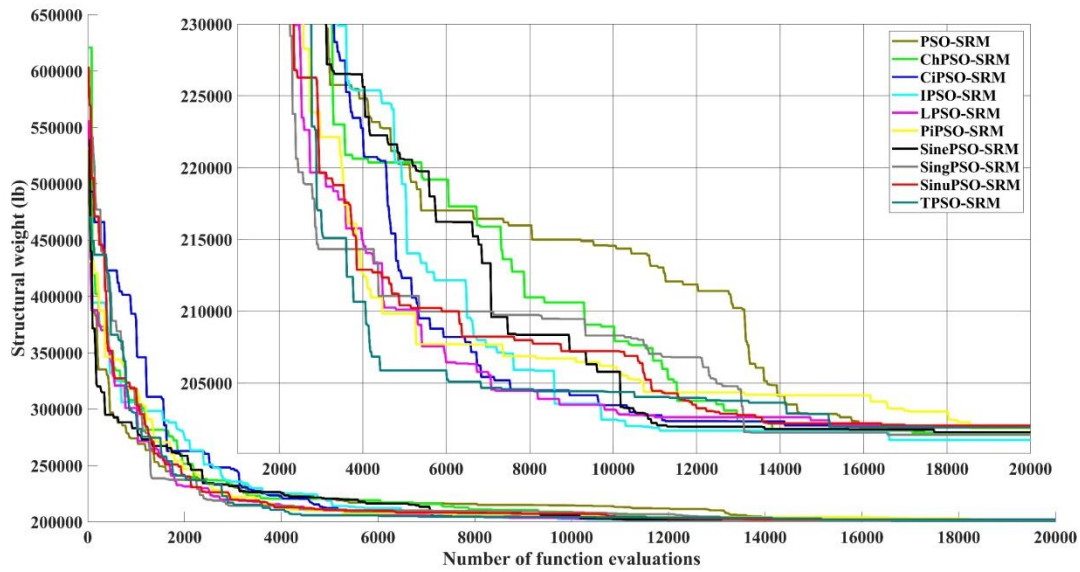


Figure 9. Convergence histories for the best run of the PSO-SRM and chaotic algorithms for the 3-bay 24-story steel frame

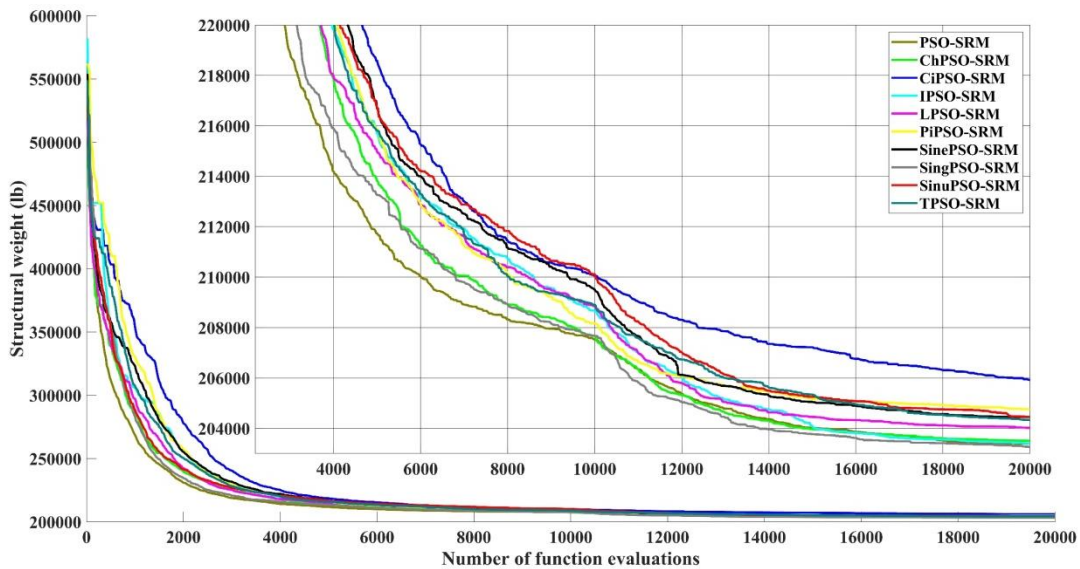


Figure 10. Convergence histories for the average run of the PSO-SRM and chaotic algorithms for the 3-bay 24-story steel frame

5. CONCLUSION

The chaotic variants of the particle swarm optimization-statistical regeneration mechanism (PSO-SRM) are presented in this paper. In these methods, chaotic maps are utilized to define the solution generation method. Nine chaotic maps, including the Chebyshev, Circle, Iterative, Logistic, Piecewise, Sine, Singer, Sinusoidal, and Tent, are applied in this study.

The performance of the chaotic variants of the PSO-SRM is tested in the three steel frame design problems. In the first example, the chaotic methods can find optimum results like the PSO-SRM. However, the statistical results of the chaotic algorithms are better than PSO-SRM. SinePSO-SRM is acquired as the optimum solution in the second example, which is better than other chaotic methods. In addition, the statistical results of the ChPSO-SRM are better than other methods. In the last example, IPSO-SRM and SingPSO-SRM can find better results than other chaotic algorithms. This result shows that the chaotic maps perfectly improve the performance of the PSO-SRM algorithms.

REFERENCES

1. Kaveh A. *Advances in metaheuristic algorithms for optimal design of structures*. 3rd edition, 2021: Springer.
2. Kaveh A, and Zaerreza A. *Structural Optimization Using Shuffled Shepherd Meta-Heuristic Algorithm: Extensions and Applications*. Studies in Systems, Decision and Control. 2023: Springer Cham.
3. Kaveh A, and Javadi SM. Shape and size optimization of trusses with multiple frequency constraints using harmony search and ray optimizer for enhancing the particle swarm optimization algorithm. *Acta Mech*, 2014. **225**(6):1595-605.
4. Kaveh A, and Zakian P. Enhanced bat algorithm for optimal design of skeletal structures. *Asian J Civil Eng (Build Hous)*, 2014.**15**(2):179-212.
5. Kaveh A, and Zaerreza A. A new framework for reliability-based design optimization using metaheuristic algorithms. *Structures*, 2022. **38**:1210-25.
6. Wu G. Across neighborhood search for numerical optimization. *Inform Sci*, 2016. **329**:597-618.
7. Almonacid B, and Soto R. Andean Condor Algorithm for cell formation problems. *Natural Comput*, 2019. **18**(2):351-81.
8. Anita and Yadav A. *AEFA: Artificial electric field algorithm for global optimization*. *Swarm Evolution Comput*, 2019. **48**:93-108.
9. Klein CE, Mariani VC, and dos Santos Coelho L. Cheetah Based Optimization Algorithm: A Novel Swarm Intelligence Paradigm. in *ESANN*. 2018. Bruges, Belgium.
10. Pierezan J, and Coelho LDS. Coyote Optimization Algorithm: A New Metaheuristic for Global Optimization Problems. in *2018 IEEE Congress on Evolutionary Computation (CEC)*. 2018.
11. Harifi S., et al., Emperor Penguins Colony: a new metaheuristic algorithm for optimization. *Evolut Intellig*, 2019. **12**(2):211-26.
12. Tahani M. and N. Babayan, Flow Regime Algorithm (FRA): a physics-based meta-heuristics algorithm. *Knowl Inform Syst*, 2019. **60**(2):1001-38.
13. Yang Y., et al., Hunger games search: Visions, conception, implementation, deep analysis, perspectives, and towards performance shifts. *Expert Syst Appl*, 2021. **177**:114864.
14. Wang G.-G., S. Deb, and Z. Cui, Monarch butterfly optimization. *Neural Comput Appl*, 2019. **31**(7):1995-2014.
15. Gholizadeh S., Danesh M, and Gheytratmand C. A new Newton metaheuristic algorithm

- for discrete performance-based design optimization of steel moment frames. *Comput Struct*, 2020. **234**:106-250.
16. Rajakumar BR. Lion Algorithm and Its Applications, in *Frontier Applications of Nature Inspired Computation*, M. Khosravy, et al., Editors. 2020, Springer Singapore: Singapore.100-18.
 17. Kallioras NA, Lagaros ND, and Avtzis DN. Pity beetle algorithm – A new metaheuristic inspired by the behavior of bark beetles. *Adv Eng Softw*, 2018. **121**:147-66.
 18. Kaveh A. and A. Zaerreza, Shuffled shepherd optimization method: a new Metaheuristic algorithm. *Eng Comput*, 2020. **37**(7):2357-89.
 19. Jain M., V. Singh, and A. Rani, A novel nature-inspired algorithm for optimization: Squirrel search algorithm. *Swarm Evol Comput*, 2019. **44**:148-75.
 20. Mahmoodabadi, M.J., M. Rasekh, and T. Zohari, TGA: Team game algorithm. *Future Comput Inform J*, 2018. **3**(2):191-9.
 21. Zhang J, et al., *Queuing search algorithm: A novel metaheuristic algorithm for solving engineering optimization problems*. *Appl Math Model*, 2018. **63**:464-90.
 22. Kaveh A. and Talatahari S. An enhanced charged system search for configuration optimization using the concept of fields of forces. *Struct Multidiscip Optim*, 2011. **43**(3):339-51.
 23. Mohebian P., Motahari MR, and Rahami H. Damage detection in retaining wall structures through a finite element model updating approach. *Asian J Civil Eng*, 2023.
 24. Al Thobiani F, et al., A hybrid PSO and Grey Wolf Optimization algorithm for static and dynamic crack identification. *Theoret Appl Fract Mech*, 2022. **118**:103213.
 25. Kaveh A. and Rahami H. Analysis, design and optimization of structures using force method and genetic algorithm. *Int J Numer Methods Eng*, 2006. **65**(10):1570-84.
 26. Kazemzadeh Azad S, Hasançebi O, and Kazemzadeh Azad S. Upper bound strategy for metaheuristic based design optimization of steel frames. *Adv Eng Softw*, 2013. **57**:19-32.
 27. Alkayem NF, et al., Inverse Analysis of Structural Damage Based on the Modal Kinetic and Strain Energies with the Novel Oppositional Unified Particle Swarm Gradient-Based Optimizer. *Appl Sci*, 2022. **12**(22):11689.
 28. Kaveh A. and Yousefpour H. Comparison of Three Chaotic Meta-heuristic Algorithms for the Optimal Design of Truss Structures with Frequency Constraints. *Period Polytech Civil Eng*, 2023.
 29. Talatahari S, Kaveh A, and Sheikholeslami R. Engineering design optimization using chaotic enhanced charged system search algorithms. *Acta Mech*, 2012. **223**(10):2269-85.
 30. Kaveh, A. and H. Yousefpour, Chaotically Enhanced Meta-Heuristic Algorithms for Optimal Design of Truss Structures with Frequency Constraints. *Period Polytech Civil Eng*, 2022. **66**(3):900-21.
 31. Gharehchopogh FS, Maleki I, and Dizaji ZA. Chaotic vortex search algorithm: metaheuristic algorithm for feature selection. *Evol Intel*, 2022. **15**(3):1777-808.
 32. Das S, and Saha P. Performance of swarm intelligence based chaotic meta-heuristic algorithms in civil structural health monitoring. *Measurement*, 2021. **169**:108533.
 33. Talatahari S, Kaveh A, and Sheikholeslami R. Chaotic imperialist competitive algorithm for optimum design of truss structures. *Struct Multidiscip Optim*, 2012. **46**(3):355-367.
 34. Kaveh A. and Javadi SM. Chaos-based firefly algorithms for optimization of cyclically large-size braced steel domes with multiple frequency constraints. *Computers &*

- Structures*, 2019. **214**:28-39.
35. Kaveh A. and Zaerreza A. Comparison of the graph-theoretical force method and displacement method for optimal design of frame structures. *Structures*, 2022. **43**:1145-59.
 36. Kaveh A. and Zaerreza A. Enhanced Rao Algorithms for Optimization of the Structures Considering the Deterministic and Probabilistic Constraints. *Period Polytech Civil Eng*, 2022. **66**(3):694-709.
 37. Wang N, Liu L, and Liu L. *Genetic algorithm in chaos*. *Or Trans*, 2001. **5**(3):1-10.
 38. Yang L.J. and Chen TL. Application of chaos in genetic algorithms. *Communications in Theoretical Physics*, 2002. **38**:168-72.
 39. Zhenyu G, et al. *Self-Adaptive Chaos Differential Evolution*. in *Advances in Natural Computation*. 2006. Berlin, Heidelberg: Springer Berlin Heidelberg.
 40. Saremi S., Mirjalili SM, and Mirjalili S. Chaotic Krill Herd Optimization Algorithm. *Proced Technol*, 2014. **12**:180-5.
 41. Wang G-G, et al., Chaotic Krill Herd algorithm. *Information Sciences*, 2014. **274**:17-34.
 42. Simon, D. Biogeography-Based Optimization. *IEEE Trans Evolutionary Comput*, 2008. **12**(6):702-13.
 43. Du D, Simon D, and Ergezer M. Biogeography-based optimization combined with evolutionary strategy and immigration refusal. in *2009 IEEE International Conference on Systems, Man and Cybernetics*. 2009.
 44. Bhattacharya A, and Chattopadhyay PK. Hybrid Differential Evolution With Biogeography-Based Optimization for Solution of Economic Load Dispatch. *IEEE Trans Power Syst*, 2010. **25**(4):1955-64.